Preprint typeset using LaTeX style emulateapj v. 10/09/06

CIRCUMSTELLAR SHELLS IN ABSORPTION IN TYPE IA SUPERNOVAE

Kazimierz J. Borkowski,[1] John M. Blondin,[1] & Stephen P. Reynolds[1]

Accepted for publication in ApJ Letters on May 22, 2009

ABSTRACT

Progenitors of Type Ia supernovae (SNe) have been predicted to modify their ambient circumstellar (CSM) and interstellar environments through the action of their powerful winds. While there is X-ray and optical evidence for circumstellar interaction in several remnants of Type Ia SNe, widespread evidence for such interaction in Type Ia SNe themselves has been lacking. We consider prospects for the detection of CSM shells that have been predicted to be common around Type Ia SNe. Such shells are most easily detected in Na I absorption lines. Variable (declining) absorption is expected to occur soon after the explosion, primarily during the SN rise time, for shells located within $\sim$ 1–10 pc of a SN. The distance of the shell from the SN can be determined by measuring the time scale for line variability.

Subject headings: ISM: bubbles — supernovae: general

1. CSM SHELLS AROUND TYPE IA PROGENITORS

Type Ia supernovae (SNe) play an important role in many areas of astrophysics, even though their progenitor systems and detailed explosion mechanisms are poorly understood. One fundamental problem involves the prediction from many models, but so far nondetection, of substantial circumstellar material (CSM), likely in the form of shells at pc-scale distances. Here, we predict the decrease in Na I absorption at early times that such shells should produce, a companion effect to Na absorption increases seen somewhat later (Patat et al. 2007a).

Most popular current Type Ia scenarios involve single degenerate ("SD") progenitors, where the donor star supplies mass to the white dwarf (WD), driving it close to the Chandrasekhar limit, where instabilities produce an explosion. A crucial step in this process is the ability of an accreting white dwarf to expel material accumulating on its surface in excess of a critical accretion rate through a fast ($v_w \sim 1000$ km s^{-1}) radiatively driven stellar outflow (Hachisu et al. 1996, 1999a,b). In the absence of such a wind, formation of a common envelope around the progenitor system is unavoidable because of the expansion of the WD envelope. The companion then merges with the white dwarf, preventing an explosion.

The WD accretion winds are expected to have profound consequences on the CSM and interstellar medium (ISM) around Type Ia SNe. Fast and powerful winds not only sweep denser CSM out of the progenitor system, they have also been suggested to strip material from the donor star (e.g., Hachisu et al. 2008) which then could form an asymmetric disk in the binary orbital plane. When swept by the SN blast wave, this material would be expected to produce high velocity absorption features, and perhaps detectable radio and X-ray emission. Farther out, the white dwarf wind blows up large-scale bubbles in the ambient ISM. Badenes et al. (2007) investigated the evolution of these bubbles with one-dimensional hydrodynamical simulations. For an ISM hydrogen density n_0 of 0.43 cm^{-3} ($\rho_0 = 10^{-24}$ g cm^{-3}) and $v_w = 10^3$ km s^{-1}, large (> 15 pc) bubbles are blown by progenitor winds, sweeping the ambient ISM into massive ($> 300\ M_\odot$) shells.

Since typical progenitor space velocities v_* of ~ 20 km s^{-1} are larger than final shell velocities, a SN explosion generally occurs after the progenitor has moved away from the bubble's center, by a distance depending on n_0 and on the progenitor scenario under consideration. If the WD explodes early ($\sim 5 \times 10^5$ yr) after the onset of the WD wind (as in models H1 and HP3 of Badenes et al. 2007), the explosion occurs off-center but still inside the bubble. For $n_0 = 0.43$ cm^{-3} and $v_* = 20$ km s^{-1}, the bubble's radius is 17 (22) pc for model H1 (HP3), while the SN exploded 7 (9) pc away from the shell. The SN would be deeper inside the bubble for slower moving progenitors and less dense ambient ISM. For faster progenitors and denser ISM, an explosion could even occur outside the bubble, but still in the vicinity of the swept-up shell.

Stellar motions are most important for progenitors that explode long after the onset and cessation of the wind (2×10^6 and 10^6 yr, respectively, in models HP1 and L2 of Badenes et al. 2007). A progenitor with $v_* = 20$ km s^{-1} travels 40 pc in 2×10^6 yr, beyond bubbles with a radius of 27 (36) pc in model HP1 (L2) (for $n_0 = 0.43$ cm^{-3}). Without a fast wind blowing at the time of the explosion, these SNe explode in the undisturbed ISM.

Another outcome is expected for a progenitor with a moderate, long-duration wind that is still blowing when the SN explodes (as in models L1 and LV1 of Badenes et al. 2007). Even if the progenitor left the bubble's interior, the wind interaction with the ambient ISM leads to the formation of a bow shock ahead of the moving SN progenitor (e.g., Wilkin 1996). The standoff distance R_0 of the swept-up ISM shell in the direction of the stellar motion is 0.75 pc for a mass-loss rate $\dot{M}_w = 10^{-7} M_\odot$ yr^{-1}, $v_w \sim 10^3$ km s^{-1}, $v_* = 20$ km s^{-1}, and $n_0 = 1$ cm^{-3} ($R_0 \propto \dot{M}_w^{1/2} v_w^{1/2} n_0^{-1/2} v_*^{-1}$). The distance to the shell is 1.3 pc in the plane perpendicular to the stellar motion direction and passing through the progenitor. The shell surface density is $\sim R_0 n_0$ ($= 2.3 \times 10^{18}$ cm^{-2} for $R_0 = 0.75$ pc and $n_0 = 1$ cm^{-3}; Wilkin 1996; Comerón & Kaper 1998). As discussed next, such a CSM shell and more massive CSM shells swept up by the

[1] Physics Department, North Carolina State U., Raleigh, NC 27695-8202; kborkow@ncsu.edu

WD winds are expected to produce detectable absorption lines in SN spectra.

CSM has also been revealed by young Type Ia supernova remnants (SNRs). Kepler's SN was a Type Ia explosion within a dense CSM (Reynolds et al. 2007). The total shocked CSM mass in Kepler's SNR is $\sim 0.75 M_\odot$ (Blair et al. 2007). The blast wave propagated to 2 pc away from the explosion center, and it is still encountering dense material with a preshock density of ~ 5 cm^{-3}. This CSM was ejected by the SN progenitor, unlike the massive swept-up ISM shells just discussed. We generally expect shells at small radii to be dominated by ejected CSM, with the swept-up ISM dominating at large radii.

2. A SIMPLE CSM SHELL MODEL

A geometrically thin, spherically symmetric CSM shell with radius R_s and mass M_s has a hydrogen column density

$$N(H) = 1.78 \times 10^{18} \left(\frac{R_s}{2 \text{ pc}}\right)^{-2} \frac{M_s}{M_\odot} \text{ cm}^{-2}. \quad (1)$$

For a shell swept up by a progenitor WD wind in a uniform ISM with density n_0, equation (1) becomes

$$N(H) = 2.06 \times 10^{18} \frac{R_s}{2 \text{ pc}} \frac{n_0}{\text{cm}^{-3}} \text{ cm}^{-2}. \quad (2)$$

Theoretical considerations and observational evidence suggest a wide range in shell masses, from a fraction of a solar mass at sub-pc scales to hundreds of solar masses at ~ 10 pc scales (Section 1). This simple CSM shell model does not encompass progenitors that left the ambient ISM undisturbed.

Shells with N(H) $\sim 10^{18}$–10^{19} cm^{-2} (eqs. 1 and 2) can be most easily detected in optical Na I and Ca II absorption lines. We focus on Na I lines, because of the likely depletion of Ca onto dust that may reduce Ca II absorption below detectable levels. The CSM dust found in Kepler (Blair et al. 2007), for example, would result in significant depletion of Ca. Neutral Na is quickly ionized by the Galactic UV radiation field because of its low (5.14 eV) ionization potential. For the "standard" UV field (e.g., Pequignot & Aldrovandi 1986), the ionization rate Γ(Na I) is equal to 1.0×10^{-11} s^{-1}. As in the general ISM, the Na ionization state is determined by the balance between ionizations and recombinations, $n(\text{Na I})\Gamma(\text{Na I}) = n_e n(\text{Na II})\, \alpha_{NaII}(T_e)$, where α_{NaII} is the recombination coefficient for Na II. For gas with predominantly singly ionized Na with a solar (cosmic) abundance of 2.0×10^{-6} (by number with respect to H; Lodders et al. 2009) and "standard" Galactic UV radiation field, N(Na I)/N(H)= $2.2 \times 10^{-7} n_e \alpha_{\rm NaII}(T_e)/\alpha_{\rm NaII}(10^3 K)$, and

$$N(\text{NaI}) = \quad (3)$$
$$3.9 \times 10^{10} \frac{\alpha_{\rm NaII}(T_e)}{\alpha_{\rm NaII}(10^3 K)} \frac{n_e}{0.1 \text{ cm}^{-3}} \left(\frac{R_s}{2 \text{ pc}}\right)^{-2} \frac{M_s}{M_\odot} \text{ cm}^{-2}.$$

For a shell swept up by the progenitor WD wind,

$$N(\text{NaI}) = \quad (4)$$
$$4.6 \times 10^{10} \frac{\alpha_{\rm NaII}(T_e)}{\alpha_{\rm NaII}(10^3 K)} \frac{n_e}{0.1 \text{ cm}^{-3}} \frac{R_s}{2 \text{ pc}} \frac{n_0}{\text{cm}^{-3}} \text{ cm}^{-2}.$$

The electron density n_e (and to a lesser degree also the electron temperature T_e) within the CSM shell are additional parameters that control the abundances of trace ions such as Na I and Ca II. Here, some degree of ionization of H produces the free electrons that permit the existence of neutral Na. A modest photon ionizing flux, provided by a SN progenitor or by the ambient extreme UV Galactic radiation field, is likely to ionize a small (~ 0.1) fraction of H atoms, so the compressed shell gas at typical densities of ~ 1 cm^{-3} (Badenes et al. 2007) is expected to be detectable in Na I lines.

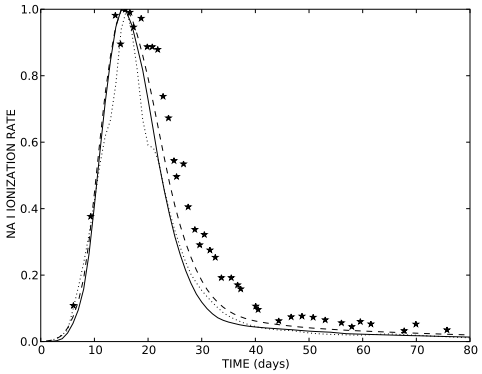

FIG. 1.— Normalized Na I ionization rate as a function of time since explosion (solid line: based on spectral templates of Nugent et al. 2002; dotted line: on the SNLS templates). A synthetic *Swift uvw2* light curve (dashed line; based on Nugent et al. 2002), and normalized *uvw2* fluxes of SN 2007af (stars) are also plotted.

In the SD progenitor scenario, ionizing photons are produced by the WD and its accretion disk. For example, Chugai (2008) considered a blackbody with $T = 3 \times 10^4$ K and $L = 300 L_\odot$ as an ionizing source in his considerations of absorption lines in SNe with symbiotic progenitors. Such a modest luminosity source is capable of significant ionization of the ambient gas to large distances away from the progenitor. We demonstrate this by performing photoionization calculations with Cloudy (ver. 08.00; Ferland et al. 1998). In addition to the blackbody radiation produced by the progenitor, we also include the diffuse Galactic UV radiation field (Draine & Bertoldi 1996) that is responsible for the ionization of Na I. A CSM shell with 1 $M_\odot$, $R_s = 2$ pc, and $n = 5$ cm^{-3} becomes nearly completely (99%) ionized by the progenitor radiation. But Na remains singly ionized, leading to an appreciable (5×10^{10} cm^{-2}) Na I column density. For a more massive (10 $M_\odot$) and distant (10 pc) shell, the H ionization decreases to 80%; N(Na I) drops slightly to 4×10^{10} cm^{-2}. N(Na I) increases with the increasing shell mass; for 50 $M_\odot$, it is equal to 2×10^{11} cm^{-2}, while H becomes partially (49%) neutral. There are large spatial variations of the diffuse ionizing radiation in galaxies, and its penetration into the CSM shell depends strongly on the assumed geometry and dynamical history of the shell. In view of these large uncertainties, we simply use equations (3) and (4) in our estimates of Na I column densities, using n_e as a free parameter to describe the unknown ionization fraction of H in the CSM shell with density $\sim$ 1–10 cm^{-3}.

3. VARIABLE NA I ABSORPTION

Photoionization of Na I by SN photons is very efficient in the immediate ($\leq$ several $\times 10^{17}$ cm) vicinity of the SN (Chugai 2008), decreasing rapidly with distance. We considered photoionization of Na I as a function of shell location R_s and time t since the explo-

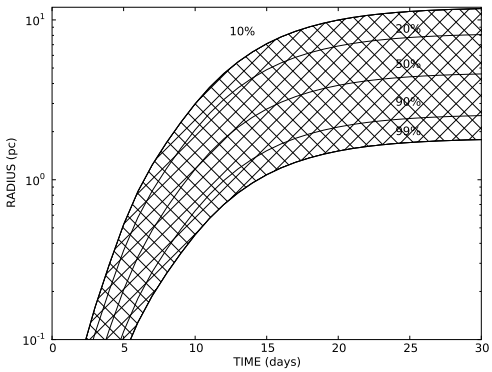

FIG. 2.— Decrease in Na I absorption as a function of time and distance from the SN. The curves are labeled by the amount of decrease in N(Na I). Reasonable prospects for the detection of absorption line variability occur within the cross-hatched area.

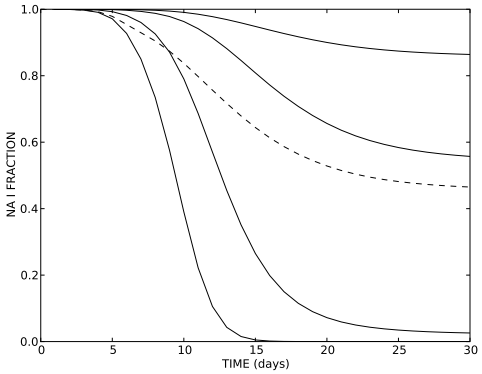

FIG. 3.— Remaining Na I fraction as a function of time since explosion for shells located at 1, 2, 5, and 10 pc (solid lines from left to right) from the SN. The dashed curve corresponding to the uniform ambient ISM is also shown.

sion, using Type Ia Branch-normal spectral templates (Nugent et al. 2002)[2] and Na I photoionization cross sections from Verner et al. (1996). Only photons with energies larger than the Na I ionization potential of 5.14 eV ($\lambda < 2410$Å) are capable of ionizing neutral sodium. Figure 1 shows the resulting Na I ionization rate as a function of time, normalized to 1 at its maximum. With $M_V = -19.46$ at maximum light (Tammann et al. 2008), the normalizing factor is equal to $3.3 \times 10^{-6}\,(R_s/2\text{ pc})^{-2}$ s^{-1}. We also show in Figure 1 the normalized Na I ionization rate based on spectral templates from the Supernova Legacy Survey (SNLS; Hsiao et al. 2007)[3]. The normalizing factor is only 7% smaller than for Nugent's templates. Flux measurements with the *Swift* satellite's *uvw2* filter ($\lambda_{central}$ = 1928Å, FWHM= 657Å) are of particular interest, since they provide light curves shortward of the Na I ionization limit. Aside from a noticeable excess at late times caused by a red leak in this filter, a synthetic *uvw2* light curve matches the Na I photoionization rate well (Figure 1). At its maximum on day 15, $M_{uvw2} = -17\overset{\text{m}}{.}5$ (using *Swift* UVOT calibration by Poole et al. 2008). For comparison, we also plot a normalized *uvw2* light curve for SN 2007af (from Brown et al. 2009), a nearby, well-observed normal Type Ia SN. We assumed a typical Type Ia rising time of 18 days (Garg et al. 2007) in the *B* band for SN 2007af. The calculated Na I ionization rate curve is narrower than the *uvw2* light curve of SN 2007af by about 3 days, while the total number of Na I ionizing photons is likely to be reasonably well modeled by the template (based on a dereddened M_{uvw2} of $-16\overset{\text{m}}{.}8$ for this SN). This modest mismatch likely reflects systematic deficiencies in our current knowledge of Type Ia UV spectra, due to their UV faintness, uncertain reddening corrections, and intrinsic UV spectral variations.

Figure 2 shows how Na I absorption decreases as a function of R_s and t, using the spectral templates of Nugent et al. (2002). Because the Na I ionization rate peaks just before the *B*-band maximum at $\sim$ 18 days (Figure 1), variable absorption is expected in the first 20–30 days after the explosion, primarily during the SN rise time. Detection will be difficult for decreases below 10% or where 99% of Na ions are ionized. Prospects for detection of variability are optimal in the middle of the cross-hatched area in Figure 2, and observational constraints favor detection of shells at pc-scale distances.

Figure 3 shows the remaining Na I fraction for shells with R_s = 1, 2, 5, and 10 pc. These curves depict variations in N(Na I) (or the equivalent width of the Na D lines in the limit of low line optical depths) as a function of time. The rate of change in absorption is much faster for shells at smaller R_s, reflecting distance-dependent ($\propto R_s^{-2}$) variations in the Na ionization rate. This sensitivity to distance from the SN can be utilized to infer distances of CSM shells from observations of absorption line variability. We also show in Figure 3 the remaining Na I fraction for uniformly (up to 10 pc) distributed ISM. Except at early times, variations in absorption are rather similar to variations produced by the shell with $R_s = 5$ pc. But absorption lines from an undisturbed ISM will be harder to detect than from the CSM shells, because these lines are more likely to be located within saturated cores of the Na I D absorption line profiles produced by the ISM in host galaxies.

Intrinsic variations in the UV among SNe are likely to affect the detectability of Na I lines. Overluminous SNe such as SN 1991T are attractive targets, because their higher than average fluxes facilitate high spectral resolution observations of absorption lines, while their potentially higher UV luminosities may allow probing of the swept-up ISM to larger distances. The brightest SNe are also associated with star-forming galaxies (e.g., Sullivan et al. 2006), implying more gas-rich environments near overluminous SNe. Conversely, subluminous SNe such as SN 1991bg are more difficult to observe, and their potentially lower UV luminosities might allow probing of the CSM only to sub-pc distances from the SN.

4. DISCUSSION

Variable Na I absorption in Type Ia SN spectra probes CSM at pc-scale distances from the SN, such as the CSM seen in Kepler's SNR. With R_s = 2 pc, $M_s = 0.75 M_\odot$, and $n_e = 0.5$ cm^{-3}, the preexplosion N(Na I) is 1.5×10^{11} cm^{-2} (from eq. 3 with $T_e = 10^3$ K). The decrease in absorption is shown in Figure 3 (second curve from left); N(Na I) drops below 10^{10} cm^{-2} on day 20. Sufficiently rapid motion (radial velocity of -230 km s^{-1}; Blair et al.

[2] Available online at www.supernova.lbl.gov/∼nugent
[3] Available online at www.astro.uvic.ca/∼hsiao

1991) of Kepler's SN progenitor would have assured no overlap with the (presumably) saturated ISM absorption in the line of sight to Kepler's SN. It is possible to measure the predicted Na I D absorption in Type Ia spectra at early times. Patat et al. (2007b) obtained a stringent (2×10^{10} cm^{-2}) upper limit for SN 2000cx. Simon et al. (2007) observed SN 2007af at three epochs (days 14, 35, and 42 in Figure 1). Their observation on day 14 was the least restrictive; the 5σ limit on the CSM absorption is 9×10^{10} cm^{-2}. The predicted column density on day 14 is 5×10^{10} cm^{-2}, at the detection limits of this observation. No detection would have been expected on days 35 and 42. Our simple shell model for Kepler is of course uncertain. Kepler's SNR is very asymmetric; depending on viewing angle, much lower or much higher column densities are possible in a SN with such strongly asymmetric CSM. Kepler's SN also has a central emission enhancement, indicating the presence of CSM at distances less than 2 pc from the SN; that would result in faster ionization by the SN.

The remnant of SN 185, SNR RCW 86, probably resulted from a Type Ia explosion within a bubble (Badenes et al. 2007). At ∼2.5 kpc away (Sollerman et al. 2003), its 21′ radius corresponds to 15 pc. Assuming a spherically symmetric bubble with this radius, the mass of the swept-up ISM is equal to $500 n_0$ $M_\odot$. From Equation (4), the preexplosion N(Na I) is larger than 10^{11} cm^{-2} for $n_0 > 0.29$ cm^{-3} (with $n_e = 0.1$ cm^{-3} and $T_e = 10^3$ K). RCW 86 is much brighter in the SW than elsewhere, suggesting an off-center explosion in this region of the SNR. The offset of the SN progenitor from the bubble's center is not known; we assume ∼ 10 pc offset from the center (∼ 5 pc distance from the shell). The decrease in absorption is shown in Figure 3 (second curve from top); half the Na atoms are ionized in the shell section closest to the SN. Significant (> 10%) variations in N(Na I) would be seen by about half of randomly distributed observers; for the other half, the CSM shell would have been too far away from the SN to produce variable absorption. The predicted column densities depend sensitively on geometric details, but our simple model for RCW 86 demonstrates that shells swept by SN progenitors should be detectable in Na I lines.

The variable Na I absorption detected in SN 2006X (Patat et al. 2007a) and SN 1999cl (Blondin et al. 2009) cannot be due to our CSM shell effect, as it is stronger, slower, and increasing rather than decreasing. While the origin of these variations is still not understood, both SNe are among the most highly reddened Type Ia SNe, leading Blondin et al. (2009) to suggest a connection to dusty environments in their host galaxies. We expect a correlation between variable absorption and the reddening within host galaxies, because formation of massive wind-swept shells at pc-scale distances from the SN can occur only in gas-rich hosts. But the line variability is confined to early times (Figure 3), and the predicted decline is obviously in conflict with the much larger increase in N(Na I) observed in SNe 2006X and 1999cl.

Typical velocities of shells swept up by the progenitor WD winds are expected to be fairly low, ∼ 10 km s^{-1}, comparable to the intrinsic velocity dispersion of the diffuse ISM, because the SN explosion usually occurs in late stages of bubble evolution after the shell has been effectively decelerated by the ambient ISM. When the shell radial velocity falls within the saturated or partially saturated Na I D line profile of the host galaxy, prospects for the shell detection are markedly reduced. This strongly favors detection of blueshifted line absorption preferentially produced by progenitors with negative radial velocities (in the host galaxy frame), comprising no more than 50% of all SNe. Another important selection effect is associated with the ambient medium density; formation of massive shells cannot occur in the low-density, hot ISM phase with a typical volume fraction of ∼ 0.5. As a result, variable absorption is expected in only a fraction (certainly no more than a quarter) of all Type Ia SNe.

Detection of variable Na I absorption from CSM shells is more difficult than for SNe 2006X and 1999cl, and requires high-resolution spectroscopy soon after a SN discovery. But such observations can map the ambient medium around many Type Ia SNe, allowing for the detection of CSM shells and establishing their distances from the SN by measuring the rate of decrease in Na I absorption. Most progenitor scenarios predict the formation of shells at pc-scale distances in many progenitor systems. This prediction can be verified by observations of variable absorption, advancing our knowledge of poorly understood Type Ia progenitors. We can learn much about these progenitors by correlating variable absorption with SN properties such as luminosities, UV excesses, or the presence or absence of high-velocity features. Observational efforts focused on high spectral resolution observations of Type Ia SNe following soon after their discovery are warranted.

We thank the referee, Nikolai Chugai, for fruitful comments on our original manuscript. This work was supported by NSF grant AST-0708224.

REFERENCES

Badenes, C., et al. 2007, ApJ, 662, 472
Blair, W. P., et al. 1991, ApJ, 366, 484
Blair, W. P., et al. 2007, ApJ, 662, 998
Blondin, S., et al. 2009, ApJ, 693, 207
Brown, P. J., et al. 2009, AJ, 137, 4517
Chugai, N. N. 2008, Astron. Lett., 34, 589
Comerón, F., & Kaper, L. 1998, A&A, 338, 273
Draine, B. T., & Bertoldi, F. 1996, ApJ, 468, 269
Ferland, G. J., et al. 1998, PASP, 110, 761
Garg, A., et al. 2007, AJ, 133, 403
Hachisu, I., et al. 1996, ApJ, 470, L97
Hachisu, I., et al. 1999a, ApJ, 522, 487
Hachisu, I., et al. 1999b, ApJ, 519, 314
Hachisu, I., et al. 2008, ApJ, 679, 1390
Hsiao, E. Y., et al. 2007, ApJ, 663, 1187
Lodders, K., et al. 2009, in Landolt-Börnstein, New Series, Astronomy and Astrophysics, (Berlin: Springer-Verlag), in press, arXiv:0901.1149
Nugent, P., et al. 2002, PASP, 114, 803
Patat, F., et al. 2007a, Science, 317, 924
Patat, F., et al. 2007b, A&A, 474, 931
Pequignot, D., & Aldrovandi, S. M. V. 1986, A&A, 161, 169
Poole, T. S., et al. 2008, MNRAS, 383, 627
Reynolds, S. P., et al. 2007, ApJ, 668, 135
Simon, J. D., et al. 2007, A&A, 474, 931
Sollerman, J., et al. 2003, A&A, 407, 249
Sullivan, M., et al. 2006, ApJ, 648, 868
Tammann, G. A., et al. 2008, A&AR, 15, 289

Verner, D. A., et al. 1996, ApJ, 465, 487
Wilkin, F. P. 1996, ApJ, 459, L31